Hindawi
Advances in Materials Science and Engineering
Volume 2023, Article ID 2386558, 10 pages
https://doi.org/10.1155/2023/2386558

Research Article

Effect of Boron Carbide Particles Addition on the Mechanical and Wear Behavior of Aluminium Alloy Composites

Ravindra,[1] M. Rajesh,[2] K. Dilip Kumar,[1] Mamunuri Sailender,[3] G. Pathalinga Prasad,[4] N. Nagaraj,[5] and Perumalla Janaki Ramulu[6]

[1]*Department of Mechanical Engineering, NMAM Institute of Technology, Affiliated to NITTE (Deemed to be University), Karkala, Karnataka-574110, India*
[2]*Department of Mechanical Engineering, Dr. Ambedkar Institute of Technology, Bengaluru, Karnataka-560056, India*
[3]*Aircraft Research and Design Centre, Hindustan Aeronautics Limited, Bangalore-560037, Karnataka, India*
[4]*Department of Mechanical Engineering, AMC College of Engineering, Bangalore-560083, Karnataka, India*
[5]*Department of Mechanical Engineering, APS Polytechnic, Bangalore 560082, Karnataka, India*
[6]*Department of Mechanical Engineering, Adama Science and Technology University, Post Box 1888, Adama, Oromia State, Ethiopia*

Correspondence should be addressed to Perumalla Janaki Ramulu; perumalla.janaki@astu.edu.et

Received 19 October 2022; Revised 22 December 2022; Accepted 7 April 2023; Published 25 April 2023

Academic Editor: Adam M. Khan

In this research, synthesis and assessment of the mechanical and wear possessions of Al7049-nano B_4C composites are determined by experiments. Using the liquid metallurgy route, a stir casting technique was used to create composites with increasing concentrations of nano B_4C from 3 to 9 weight %. Each composite's reinforcement particles were heated to 400 degrees Celsius before being added to the molten Al7049 alloy in two separate steps, i.e., two-stage stir casting to optimise wettability and distribution. Scanning electron microscopy (SEM) was utilised to examine the microstructure, and energy dispersive spectroscopy (EDS) was utilised to determine the elemental make-up. Mechanical characteristics of composites were determined by subjecting them to tensile, compression, and hardness tests. Wear tests were conducted as per ASTM G99 standards with varying loads and speeds. Nanosized B_4C particles were found to be dispersed throughout the sample space in a microstructural analysis. Hardness, ultimate strength, yield strength, and compression strength of Al7049 alloy composites were found to increase significantly as the weight percentage of nano B_4C was increased. Additionally, compared to the unreinforced form, the ductility of the Al7049 alloy composites was slightly reduced. SEM micrographs of tensile-fractured specimens were used for research into the field of tensile fractography. Nano B_4C reinforced composites exhibited superior wear resistance as compared to Al7049 alloy. These prepared composites can be used for wing root fitting of an aircraft.

1. Introduction

The phenomenon of passivation gives aluminium its remarkable corrosion resistance. Due to its high strength to weight ratio, ease of machinability & formability, and lower cost relative to other materials [1, 2], aluminium and its alloys are indispensable to the automotive and aerospace industries. There is a lot of work being done to improve the strength-to-weight ratio of aluminium alloys by combining very high strength materials as reinforcement. The mechanical possessions can be modified as desired by adding reinforcement materials. Metal matrix composites (MMC) are a relatively new material that emerged as a result of the fusion of reinforcing materials with base materials such as aluminium alloy.

Even though the availability of many kinds of reinforcing and matrix materials is there, an effort is made to fabricate the composite material with aluminium alloy as base material and boron carbide (B_4C) as reinforcing particulate material [3]. The reinforcement B_4C

particulate material is varied in weight percentages with respect to the matrix alloy and specimens are produced to compare for their properties.

More prominent metal matrix composite is aluminium based metal matrix composite (AMMC) that is why many of researchers trying to invent better and better aluminium metal matrix composite for their engineering components [4]. One can come to a understanding about the aluminium metal matrix composite (AMMC) that usage and producibility or manufacturability of aluminium alloy metal matrix composite from the recent research papers presented all over the world. While finalizing this material for research, factors considered are the type of engineering parts, working environment, way of fabrication, cost, nature of reinforcing material and its shape, size, its distribution [5].

Alloys of aluminium generally will have aluminium as major element and small constituents such as copper, silicon, manganese, magnesium, as alloying elements. These aluminium alloys are classified into many series on the basis of various combination of above said alloying elements. These aluminium alloys are having major advantage of strength to weight ratio in comparison with steel, iron, copper, and brass, and other properties, such as corrosion, wear resistance, and ductility, are also made aluminium alloys more popular particularly when compared with the steel or iron weight of aluminium is approximately 64% less by weight.

Besides finalizing the aluminium alloys metal matrix composite, the type of aluminium alloys material selected is 7XXX aluminium alloy. In 7XXX series alloy, zinc is the main alloying constituent united with magnesium for strengthening.

Recent studies have shown that adding ceramic particles to a material can increase its wear resistance and help improve its mechanical properties, even when exposed to high temperatures. A matrix's ability to resist deformation, carry weight, and lock microcracks along the friction direction is greatly enhanced by the presence of B_4C.

The production methods of Al7049/B_4C combinations can be categorized into three types: solid state method, liquid state, and semisolid-state method. The solid-state strategy can be isolated into powder metallurgy, mechanical alloying, and dispersion holding strategies. Contrasted with different courses, dissolve mixing procedure has some significant focal points, e.g., the wide choice of materials, better framework molecule holding, simpler control of grid structure, basic and reasonable preparing, and adaptability to huge amount creation and brilliant profitability for close net formed parts [6, 7]. Be that as it may, there are a few issues related with mix giving of metal composites such a role as poor and heterogeneous appropriation of the support material. Improvement in wettability to certain degree can be accomplished by a few techniques such as expansion of halide salts, mechanical blending, preheating the support particles to expel the retained gases from the molecule surface, expansion of alloying components such as Mg, Zr, and Si_3N_4, and utilization of surface coatings on fortification molecule and so forth [8].

It would be fascinating to learn more about the mechanical properties of aluminium alloys that have been strengthened by nano hard boron carbide. Therefore, the purpose of the existing investigation is to develop a stir casting method for the synthesis of Al7049-B_4C metal matrix composites utilising nanoparticles. 500 nm B_4C particles are intended for use in this study. Furthermore, mechanical and wear properties of the prepared composites will be assessed in accordance with ASTM standards. Based on the literature, it is difficult to distribute the particles uniformly in the matrix, hence to enhance the wettability between the Al7049 matrix and nano boron carbide particles. A novel two-stage stir casting method is adopted to prepare the nanocomposites. In this process, entire reinforcement is added to the melt in two stages instead of adding at one stage which helps to improve the interfacial bonding.

This study was conducted to analyze the effects of nano B_4C on the microstructure, mechanical belongings, and wear resistance of Al7049 alloy. For this reason, AMCs will be produced using the stir method. Nano B_4C's influence on the composite's hardness, tensile, and compression behavior is studied. Scanning electron microscopy (SEM) is used to analyze the particle distribution and fractography of the specimen's microstructures.

2. Experimental Details

2.1. Materials. The matrix substantial in this investigation is Al7049, an aluminium-zinc alloy that is widely used in industries such as aerospace, automobiles, and the oceanic sector. Zinc content in Al7049 is typically 7.8% (Table 1). Al7049 has an assumed theoretical density of 2.84 g/cm^3.

Reinforcing materials in this work are nanoscale B_4C particulates; specifically, 500 nm. Boron carbide has a lower density than the matrix material (2.52 g/cm^3). Figure 1 is the SEM micrograph of 500 nm boron carbide particles.

2.2. Preparation of Nanocomposites. The Al7049-B_4C composites were made using a stir casting technique and the liquid metallurgy route. A precise number of ingots of Al7049 alloy are loaded into the melting furnace. Aluminium alloy has a melting point of 660 degrees Celsius. The molten substance reached a superheated temperature of 750 degrees Celsius. A chromel-alumel thermocouple was used to take the readings. After that, solid hexachloroethane (C_2Cl_6) [9] is used to degas the molten metal for three minutes. A zirconium-coated stainless steel impeller is used to create a vortex in the molten metal by stirring the material. Impeller immersion depth was 60% of the melt's height, and the stirrer would be rotated at 300 rpm. In addition, B_4C particles that have been preheated to temperatures of up to 400°C will be injected into the vortex in two stages to improve the wettability. To encourage wetting, stirring must be maintained until the reinforcement particulates interact with the matrix at their interface. The Al7049-3 wt.% of nano B_4C mixture is then poured into a 120 mm length and 15 mm diameter permanent cast iron mould. Composites are also made

Table 1: Chemical composition of Al7049 Alloy.

Element	Si	Cu	Mg	Mn	Fe	Zn	Cr	Ti	Al
Wt. (%)	0.23	1.5	2.5	0.20	0.30	7.8	0.15	0.10	Balance

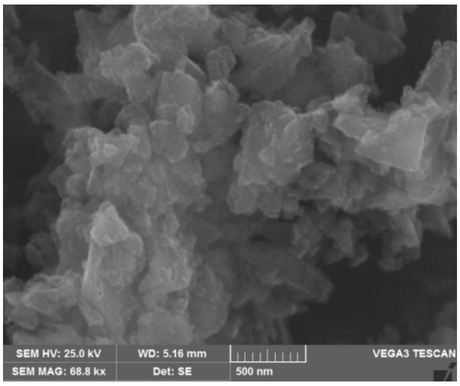

Figure 1: SEM micrograph of nano B_4C particles.

with different percentages of nano B_4C particles. Figure 2 is representing Al7049 with B_4C nanocomposite after casting.

2.3. Evaluation of Properties. To obtain the required sample piece for microstructure study, the castings acquired were cut to proper size, measuring 15 mm in diameter and 5 mm in thickness, and then polished to varying degrees. Before moving on to polishing with Al_2O_3 suspension on a polishing disc using velvet cloth, the sliced samples were first polished with emery paper up to 1000 grit size. Finally, a 0.3 micron diamond paste was used to polish the surface. A scanning electron microscope was used to examine the microstructure of the samples after their polished surface had been etched with Keller's reagent.

The average of three sets of readings taken from various spots on the specimens' polished surfaces was used for the final analysis. Brinell hardness testing machines were used to measure the specimens' resistance to indentation by applying a 250-kilogram load to a 5-millimeter-diameter ball indenter and letting it sit for 30 seconds. At room temperature, using an universal testing machine calibrated to ASTM E8 and E9 standards [10], the tensile strength, yield stress, percentage elongation, and compression strength of the cut specimens were determined. Figure 3(a) is a picture of the tensile test specimen.

A pin holder secures the specimen against the counter face of a disc with a 90 mm wear track diameter, which is then rotated. Wear loss required for loading the pin is calculated against the disc with 2 kg, 3 kg, and 4 kg of dead weights. Size of the specimen is depicted in Figure 3(b); it measures 30 mm in length and 8 mm in diameter as per ASTM G99 standard [11]. The disc is washed with acetone before the test, then worn samples are tested, and electronic sensors are used to record the wear. The rotating disc and its pin were flattened and cleaned extensively before the test. The next step is to set the track diameter to 90 mm and clamp the specimen in the chuck.

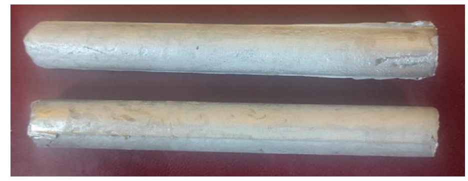

Figure 2: Al7049 with B_4C nanometal composite after casting.

3. Results and Discussion

3.1. Microstructural Study. The distribution of reinforcing particles within the matrix of the base metal can be determined from microstructural analyses along with the grain size and shape of the grains present. Both mechanical and wear properties will be significantly impacted by this study. Scanning electron microscope micrographs of B_4C particles with 500 nm reinforcements of varying percentage weights are described in Figures 4(a)–4(d).

Micrographs taken with a scanning electron microscope reveal the differences between as cast alloy Al7049 and composites comprehending 3, 6, and 9 wt.% of nano B_4C reinforced with Al7049 alloy (Figures 4(a)–4(d)). The two specimens under review here are taken from the cylindrical samples' proximal and distal midpoints. As cast, the microstructure of Al7049 alloy consists of fine grains of Al solid solution with an adequate dispersion of intermetallic precipitates.

It also demonstrates the identical standardized circulation of nanosized B_4C without agglomeration and bunching in the composites, demonstrating a strong hold between the framework and the fortification (Figure 5). This is primarily attributable to the successful mixing action carried out throughout the fort's two-stage expansion. The nanoparticles all over the lattice's grain boundary prevent the grains from improving and fight the separation of grains as they stack [12].

From Figure 5(b), it is identified that nano B_4C particles are found in the Al7049 alloy matrix in the form of B and C elements along with Al and Zn.

3.2. Hardness. The addition of 3 to 9 wt.% nano B_4C to the Al7049 alloy causes noticeable changes in hardness, as shown in Figure 6. To measure a material's resistance to local plastic deformation, a mechanical parameter known as "hardness" is used. The addition of 3, 6, and 9 wt.% nano B_4C increases the hardness of Al-B_4C composite. Al composites exhibit this improvement, going from 67.5 BHN to 98.3 BHN. This is due, in large part, to the presence of harder carbide particles in the lattice, which imposes greater constraints on the localised matrix deformation that occurs during indentation [13, 14]. As with other reinforcements, B_4C helps strengthen the matrix by creating high-density dislocations as the material cools to room temperature due to the disparity in thermal expansion coefficients between the B_4C and the grid Al7049 compound. Increasing the hardness of composites, mismatch strains between the reinforcement and matrix, prevents dislocations from moving freely.

(a) (b)

Figure 3: (a) Tensile test specimen and (b) wear test specimen.

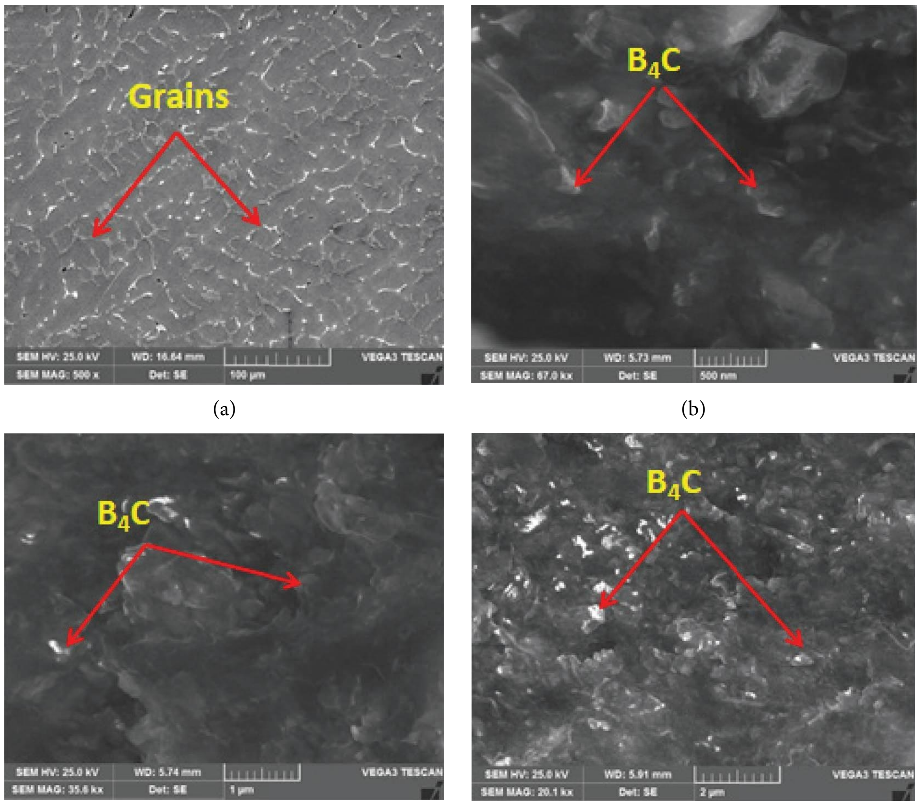

(a) (b)

(c) (d)

Figure 4: SEM images of (a) as cast Al7049 alloy, (b) Al7049 with 3% B_4C, (c) Al7049 with 6% B_4C, and (d) Al7049 with 9% B_4C composites.

Basically, strengthening particles are stronger and more rigid than the Al7049 alloy, and these strengthening particles always try to avoid the plastic deformation of the matrix throughout the testing. But avoiding the plastic deformation of the Al7049 alloy relies on the deformation of the nanoparticles in the matrix.

3.3. Ultimate Tensile Strength and Yield Strength. Figure 7 presents a plot of ultimate tensile strength (UTS) versus the percentage of nano B_4C dispersoid in a metal lattice composite. UTS was plotted as a percentage of the total weight of nano B_4C, based on careful calculations. The value of UTS has shifted by 25.78% in comparison to the standard Al7049 alloy. True contact among the framework and the auxiliary materials is credited with the strength increase. Hardness and quality of composites improve with increasing grain estimate, which in turn leads to increased wear resistance. Because of the close proximity of hard nano B_4C, the quality of the framework amalgam is enhanced, leading to increased rigidity [15, 16]. The difference in coefficient of growth between the flexible matrix and the brittle particles suggests that the growth of these particles may have significantly increased the lingering compressive anxiety during cementing. Dense packing of reinforcement and, by extension, minimal interparticle spacing in the lattice are both credited with quality improvements.

Figure 8 displays the yield strength (YS) of Al7049 alloy matrices with 3 to 9 wt.% of nano B_4C composites. The strength of the Al alloy was increased from 177.4 MPa to 195.5 MPa, 205.7 MPa, and 227.1 MPa when 3 to 9 wt.% of B_4C was added. This improvement in yield quality is consistent with findings from various specialists who have detailed how the quality of molecule-fortified composites is extremely dependent on the weight % of the fortification. When hard B_4C particles are close by, they impart quality to the soft aluminium network, increasing the composite's resistance to the applied ductile load [17, 18]. This causes the

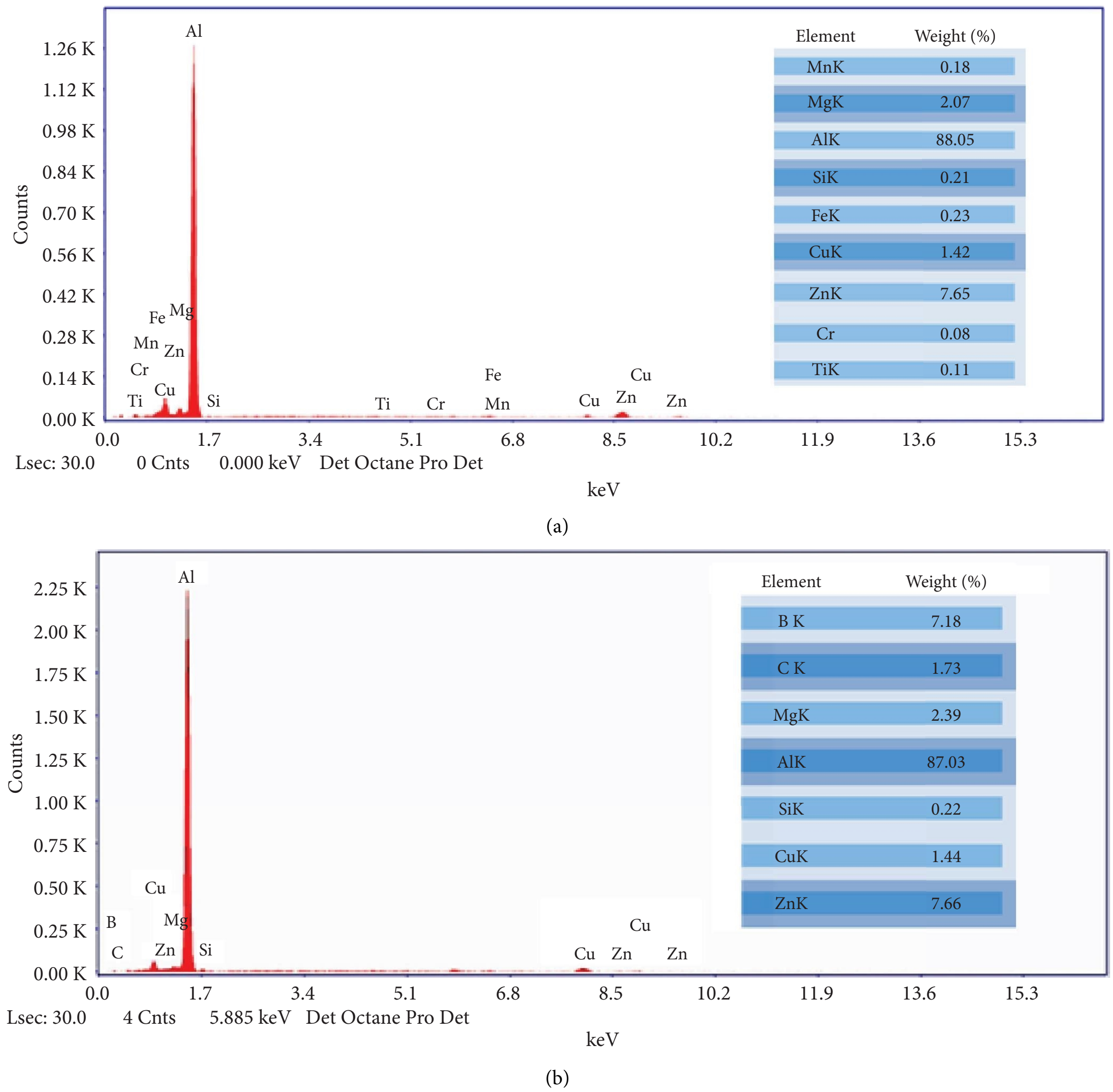

FIGURE 5: EDS spectrums of (a) as cast Al7049 alloy and (b) Al7049-9 wt.% B_4C composites.

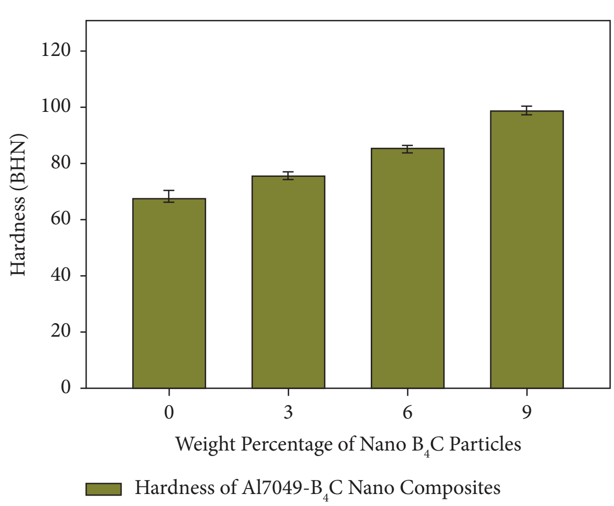

FIGURE 6: Variation in hardness of Al7049 with nano B_4C composites.

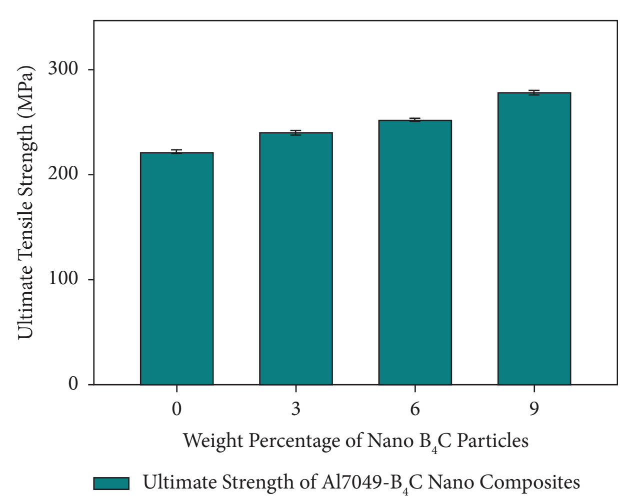

FIGURE 7: Variation in ultimate tensile strength of Al7049 with nano B_4C composites.

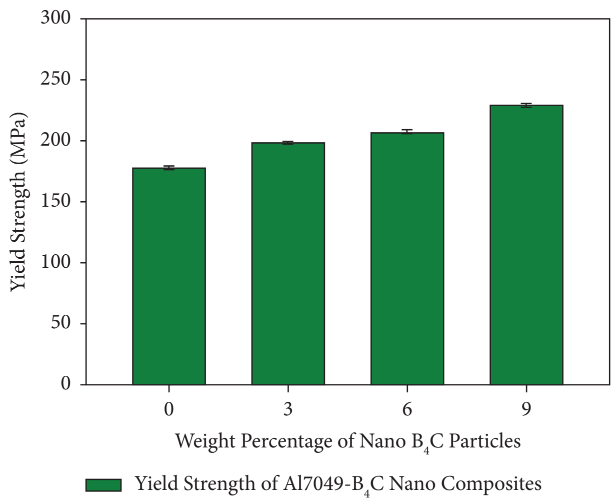

Figure 8: Variation in yield strength of Al7049 with nano B_4C composites.

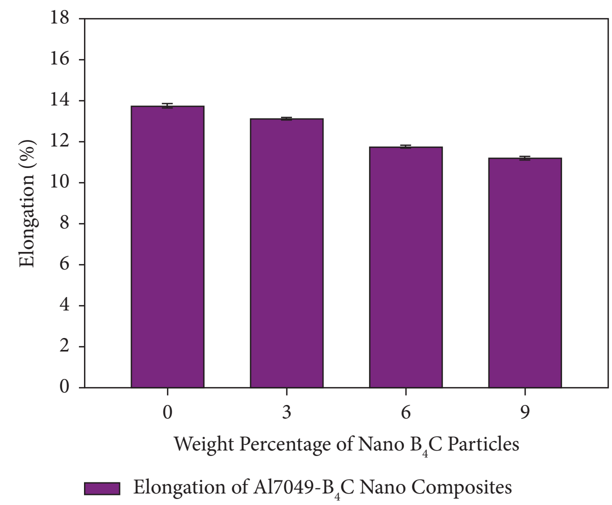

Figure 9: Variation in percentage elongation of Al7049 with nano B_4C composites.

composite's Young's modulus to grow. Molecule-enhanced composites benefit from increased quality due to the constraint of the plastic stream imposed by the dispersed hard particles in the grid.

According to Figures 7 and 8, the Al7049 matrix contains nanosized particles, which contribute significantly to the material's increased tensile strength. The addition of more boron carbide particles to the base is what causes this improvement to be seen. Due to the incorporation of reinforcing particles, the tensile strength of the Al7049 alloy is improved, as is its resistance to tensile stress. The boron carbide particles also start out with a lot of stress because the carbide particles are stiffer than the Al matrix [3, 19]. The addition of B_4C particles to the Al7049 alloy also helps to increase the work hardening of the composites due to the geometric constraints imposed by the presence of reinforcement.

3.4. Percentage Elongation. Figure 9 shows how the nano B_4C percentage affects the composites' ability to stretch (their ductility). From the graph, we can deduce that the composites fortified with 3, 6, and 9 wt.% B_4C lose a lot of their pliability. Detriment in the form of a slower rate extension relative to the base amalgam is a common occurrence in particulate-fortified metal lattice composites [20]. The presence of B_4C particulates, which can break and have sharp corners, contributes to the reduced pliability in composites and makes them more prone to limited split start and proliferation.

3.5. Compression Strength. Compression strength of Al7049 alloy matrix reinforced with 3 to 9 wt.% of nano B_4C particulate is shown in Figure 10. Compression strength of the Al alloy was found to increase from 589.6 MPa to 620.1 MPa, 670.4 MPa, and 738.5 MPa after adding 3 to 9 wt.% of B_4C particles. The addition of tough ceramic particles to the Al7049 alloy matrix is largely

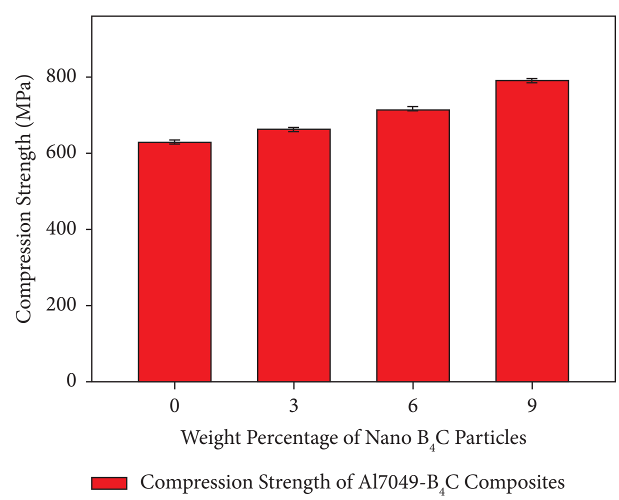

Figure 10: Variation in compression strength of Al7049 with nano B_4C composites.

responsible for the resulting boost in compression strength. Always particles strength is expressed in terms of compressive strength. Especially, boron carbide particles are very strong in compression strength; inclusion of these hard particles avoids the plastic deformation of Al7049 alloy matrix [21].

3.6. Fracture Studies. SEM images of fracture surfaces were used to investigate the mechanisms of fracture for both as cast alloy and composites subjected to tensile testing (Figures 11(a)–11(d). Figure 11(a) displays the ductile fracture mode of the as cast Al7049 alloy, which consists of an enormous number of dimple-shaped structures but no crack.

A less ductile failure is observed in the fracture structures of 3, 6, and 9 wt.% B_4C reinforced MMCs (Figures 11(b)–11(d)). Particle cracking, matrix material fracture, and debonding at the alumina particle-Al matrix alloy interface

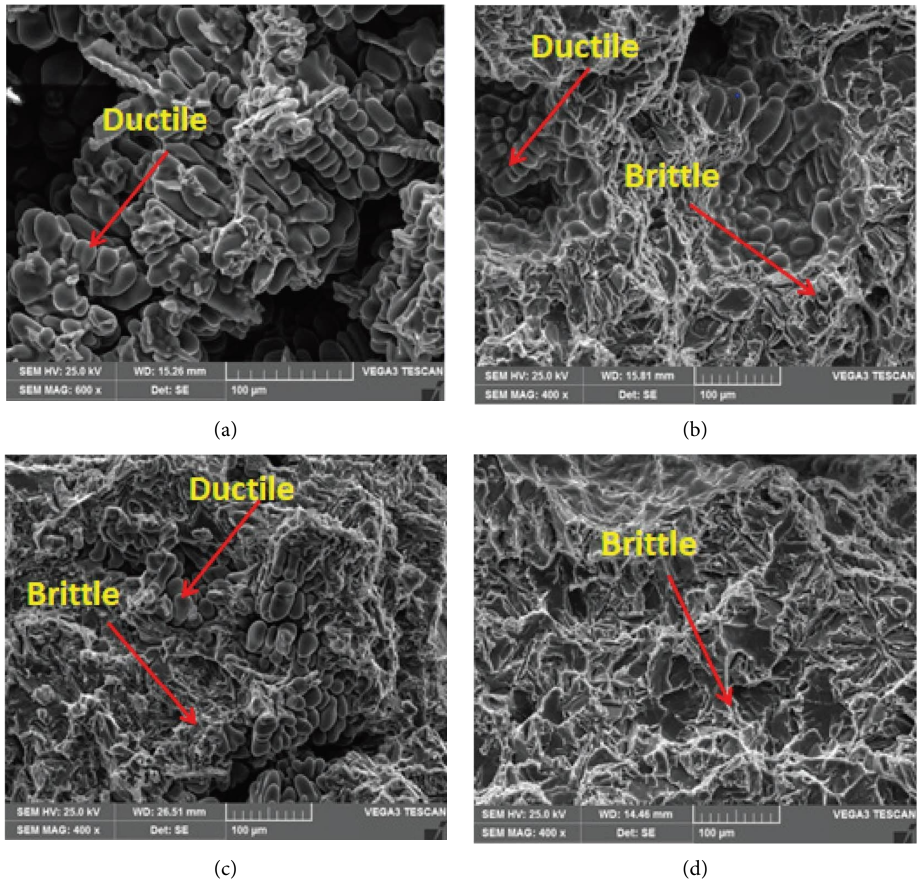

Figure 11: Tensile fractured SEM images of (a) Al7049 alloy, (b) Al7049-3 wt.% B_4C, (c) Al7049-6 wt.% B_4C, and (d) Al7049-9 wt.% B_4C composites.

are all generally accepted as contributing factors in MMC failure during tensile testing. Fracture surfaces of 9 wt.% of B_4C composites showed local stresses at the interfaces are greater, leading to a crack at the reinforcement particles.

3.7. Wear Studies. The Al7049 alloy and its nanosize B_4C reinforced composites are put through wear tests with loads ranging from 2 to 4 kg (in 1 kg increments) slid along a smooth surface at a constant speed of 400 rpm for a total of 3000 m. Experiments were also run with a constant load of 4 kg and a distance of 3000 m but with sliding speeds ranging from 200 rpm to 400 rpm in 100 rpm increments. The results of all the tests are recorded in terms of the height loss in micrometres (μm).

3.7.1. Effect of Load on Wear Loss. The load is a major factor in the rate of wear and tear. The impact of load in wear tests has been studied extensively in order to characterize the wear rate of aluminium alloys. In addition, graphs for wear loss against load of 2 kg, 3 kg, and 4 kg have been plotted at a constant distance of 3000 meters and speed of 400 rpm to analyze the impact of load on wear. As can be seen in Figure 12, the wear behavior of Al7049 alloy and B_4C composites is affected by load.

Wear increases for all composites and the base Al7049 as the load is increased from 2 kg to 4 kg, as seen in graph 12. The sliding surface and pin reach temperatures above the critical value at a maximum load of 4 kg. Consequently, wear of the matrix Al7049 alloy and Al7049 alloy-3, 6, and 9 wt.% B_4C composites increases with increasing load on the pin. As cast Al7049 alloy has the highest wear loss under all loading conditions, as shown in Figure 12, wear loss of composites is seen to decrease as reinforcements in Al7049 alloy are increased in weight percent. As the weight percentage of B_4C reinforcements in Al7049 alloy composites increases from 3 to 9, the composites' resistance to wear increases. This may be because the high hardness of B_4C acts as a barrier for the wear loss [22, 23].

3.7.2. Effect of Sliding Speed on Wear Loss. Several test samples of different compositions show wear loss as a function of speed variation in Figure 13. Experiments are run with a constant load of 4 kg and disc speeds of 200 rpm, 300 rpm, and 400 rpm. According to the data presented in the following graph, the amount of material lost due to wear and tear grows in proportion to the square of the sliding velocity. Sliding velocity has a greater impact on Al7049 alloy at its base than it does on B_4C-based composite.

Despite this, the wear of the composites is much lower compared to the Al7049 matrix alloy at all sliding speeds,

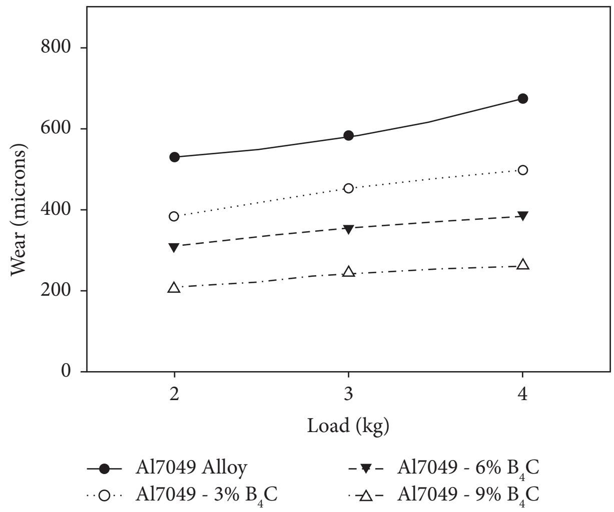

Figure 12: Wear loss of Al7049 and nanosize B_4C composites at varying loads and 400 rpm constant speed.

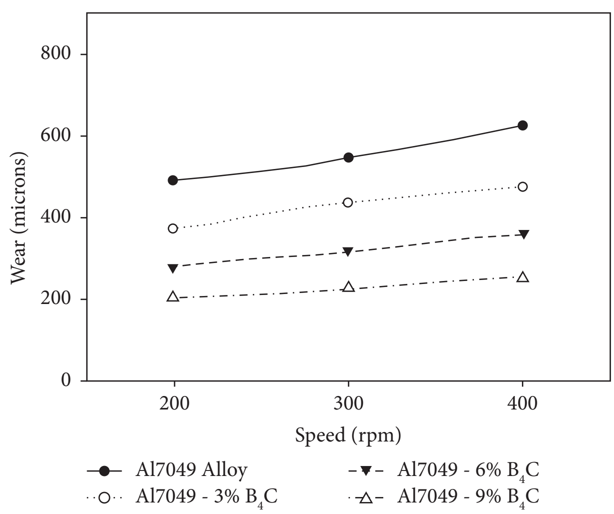

Figure 13: Wear loss of Al7049 and its nanosize B_4C composites at varying speeds and 4 kg constant load.

especially in the case of Al7049 with 3 to 9 wt.% of nano B_4C composites. Wear loss of the composite material is reduced generally speaking as the amount of B_4C particles present increases. Another reason wear increases with sliding speed is that rubbing action warms the composite and causes it to soften, leading to more loss of material [24, 25]. Due to the increase in temperature, plastic deformation of the test piece occurs at higher sliding speeds. As a result, there is more delamination, which contributes to more wear and tear. The present work's findings are consistent with and similar to those of other researchers'.

3.7.3. Wear Worn Surface Analysis. Figure 14(a) depicts the worn surface of Al7049, which exhibits the incidence of grooves, micropits, and a fractured oxide layer, all of which are likely the result of increased wear loss. Figures 14(b)–14(d) display how the presence of B_4C particles in Al7049 with 3 to 9 wt.% nano B_4C composites limits the viscous flow of the matrix, leading to a decrease in grooves or erosion and, consequently, an increase in wear resistance [26, 27]. Worn areas reveal fewer and fewer cracks and grooves as the number of B_4C particles increases, suggesting that stress is transferred to and concentrated on these particles.

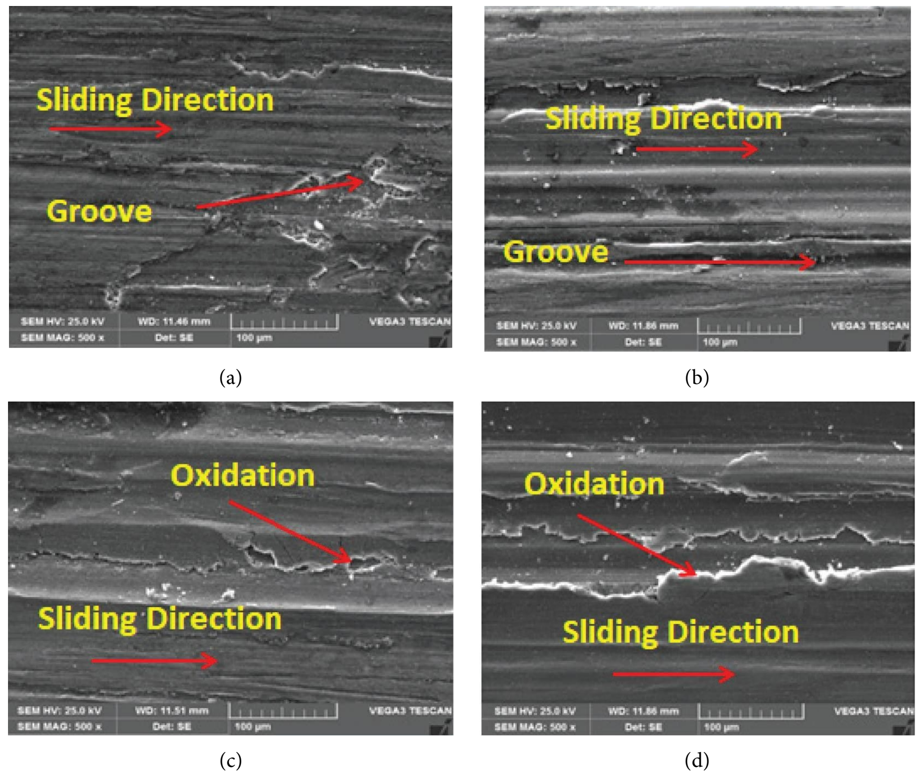

Figure 14: Worn surface SEM micrographs of (a) Al7049 alloy, (b) Al7049 with 3 wt.% B_4C, (c) Al7049 with 6 wt.% B_4C, and (d) Al7049 with 9 wt.% B_4C composites at 4 kg load and 400 rpm speed.

4. Conclusions

(i) The stir casting has been used successfully to create composites of Al7049 alloy with 3 to 9 wt.% of nanosized B_4C particulates for reinforcement.

(ii) Nanosized B_4C particles were seen to be dispersed throughout the Al7049 alloy matrix in scanning electron micrographs. Nanoparticles of B_4C, composed of the elements B and C, were found in Al7049-B_4C composites, according to energy dispersive spectroscopy analysis.

(iii) Nanoscale B_4C particles increased the hardness of Al7049 alloy composites by 3, 6, and 9 weight percent. As cast, Al7049 alloy has a hardness of 67.5 BHN; however, when strengthened with 9 wt.% B_4C composites, its hardness increases to 98.3 BHN.

(iv) The addition of the B_4C particles to the Al7049 matrix increases the material's ultimate and yield strength. By adding 9 wt.% nanosized B_4C particulates to Al7049, the ultimate strength of the composite improved from 222 MPa to 279.3 MPa. When compared to the yield strength of Al7049 alloy (177.4 MPa), the values for composites containing 3, 6, and 9 wt.% of B_4C are 197.5 MPa, 205.7 MPa, and 227.1 MPa, respectively. The elongation of Al7049 alloy is reduced when nanosized B_4C particles are added to the mix. The addition of 3 to 9 wt.% nano B_4C particulates improved the compression strength of Al7049 alloy.

(v) The wear behavior of Al7049 and its composites was found to be sensitive to both the applied load and the sliding speed. A higher load and faster speed both lead to a greater wear loss. However, nano B_4C composites with 3, 6, and 9 wt.% showed remarkable improvement in wear resistance. Micrographs of worn surfaces taken with a scanning electron microscope (SEM) revealed the varying wear mechanisms.

(vi) All the properties have been improved due to the two-stage reinforcement addition method adopted to fabricate the composites.

Data Availability

The data that support the findings of this study are available upon request from the corresponding author.

Conflicts of Interest

The authors declare that they have no conflicts of interest.

References

[1] C. Tom Scaria and R. Pugazhenthi, "Effect of process parameter on synthesizing of TiC reinforced Al7075 aluminium alloy nano composites," *Materials Today Proceedings*, vol. 37, no. 2, pp. 1978–1981, 2021.

[2] S. Basavarajappa, G. Chandramohan, A. Mahadevan, M. Thangavelu, R. Subramanian, and P. Gopalakrishnan,

"Influence of sliding speed on the dry sliding wear behaviour and the subsurface deformation on hybrid metal matrix composite," *Wear*, vol. 262, no. 7-8, pp. 1007–1012, 2007.

[3] T. H. Raju, R. S. Kumar, S. Udayashankar, and A. Gajakosh, "Influence of dual reinforcement on mechanical characteristics of hot rolled AA7075/Si3N4/graphite MMCs," *Journal of the Institution of Engineers*, vol. 102, no. 2, pp. 377–387, 2021.

[4] R. Suresh, "Comparative study on dry sliding wear behavior of mono (Al2219/B4C) and hybrid (Al2219/B4C/Gr) metal matrix composites using statistical technique," *Journal of the Mechanical Behavior of Materials*, vol. 29, no. 1, pp. 57–68, 2020.

[5] S. Dayanand, S. B. Boppana, V. Auradi, M. Nagaral, and M. Udaya Ravi, "Evaluation of wear properties of heat-treated Al-AlB2 in-situ metal matrix composites," *Journal of Bio-and Tribo-Corrosion*, vol. 7, no. 2, pp. 40–11, 2021.

[6] S. Dhanalakshmi, N. Mohanasundararaju, and P. Venkatakrishnan, "Preparation and mechanical characterization of stir cast hybrid Al7075-Al2O3-B_4C metal matrix composites," *Applied Mechanics and Materials*, vol. 592–594, pp. 705–710, 2014.

[7] L. J. Zhang, D. L. Yang, F. Qiu, J. G. Wang, and Q. C. Jiang, "Effects of reinforcement surface modification on the microstructures and tensile properties of SiCp/Al2014 composites," *Materials Science and Engineering A*, vol. 624, pp. 102–109, 2015.

[8] H. R. Ezatpour, S. A. Sajjadi, M. H. Sabzevar, A. Chaichi, and G. R. Ebrahimi, "Processing map and microstructure evaluation of AA6061-Al_2O_3 nano composite at different temperatures," *Transactions of Nonferrous Metals Society of China*, vol. 27, no. 6, pp. 1248–1256, 2017.

[9] V. Ravindranath, G. S. Shivashankar, S. Basavarajappa, and N. G. Siddesh Kumar, "Dry sliding Wear Behavior of Hybrid aluminum Metal Matrix composite reinforced with Boron carbide and graphite particles," *Materials Today Proceedings*, vol. 4, no. 10, pp. 11163–11167, 2017.

[10] G. Rajaram, S. Kumaran, and S. Suwas, "Effect of strain rate on tensile and compression behaviour of Al–Si/graphite composite," *Materials Science and Engineering A*, vol. 528, no. 19-20, pp. 6271–6278, 2011.

[11] T. Rajkumar, K. Radhakrishnan, C. Rajaganapathy, S. P. Jani, and N. Ummal Salmaan, "Experimental investigation of AA6063 welded joints using FSW," *Advances in Materials Science and Engineering*, vol. 2022, Article ID 4174210, 10 pages, 2022.

[12] H. S. Vasanth Kumar, K. Revanna, N. Kumar et al., "Impact of silicon carbide particles weight percentage on the microstructure, mechanical behaviour, and fractography of Al2014 alloy composites," *Advances in Materials Science and Engineering*, vol. 2022, Article ID 2839150, 10 pages, 2022.

[13] C. Anilkumar and H. N. Reddappa, "Studies on mechanical, wear and corrosion properties of Al6061-Beryl-Cerium Oxide hybrid metal matrix composites," *International Journal of Renewable Energy Technology*, vol. 3, no. 6, pp. 227–233, 2014.

[14] S. M. Subramanian, J. Vijayan, and V. Muthaiah, "Tribological wear behaviour and hardness measurement of SiC, Al_2O_3 reinforced Al matrix hybrid composite," *Journal of the Institution of Engineers*, 2017.

[15] N. Kumar, H. S. Kumar, T. H. Raju, M. Nagaral, V. Auradi, and R. K. Veeresha, "Microstructural characterization, mechanical and taguchi wear behavior of micro-titanium carbide particle-reinforced Al2014 alloy composites synthesized by advanced two-stage casting method," *Journal of Bio- and Tribo-Corrosion*, vol. 8, no. 4, p. 109, 2022.

[16] Y. Bai, Y. Guo, J. Li, Z. Yang, and J. Tian, "Effect of Al_2O_3 nano particle reinforcement on the mechanical and high temperature tribological behavior of Al-7075 alloy," *Proceedings of the Institution of Mechanical Engineers - Part J: Journal of Engineering Tribology*, vol. 231, no. 7, pp. 900–909, 2017.

[17] J. P. Cottu, J. J. Couderc, B. Viguier, and L. Bernard, "Influence of SiC reinforcement on precipitation and hardening of a metal matrix composite," *Journal of Materials Science*, vol. 27, no. 11, pp. 3068–3074, 1992.

[18] B. Anil Kumar, A. Ahamad, and H. N. Reddappa, "Impact of B4C reinforcement on tensile and hardness properties of Al-B4C metal matrix composites," *Materials Today: Proceedings*, vol. 52, pp. 2136–2142, 2022.

[19] M. Ravikumar and R. Nail, "Impact of nano sized SiC and Gr on mechanical properties of aerospace grade Al7075 composites," *Frattura Ed Integrità Strutturale*, vol. 16, pp. 439–447, 2022.

[20] M. Ravikumar, H. N. Reddappa, R. Suresh, E. R. Babu, and C. R. Nagaraja, "Study on micro - nano sized Al2O3 particles on mechanical, wear and fracture behavior of Al7075 Metal Matrix Composites," *Frattura Ed Integrità Strutturale*, vol. 15, no. 58, pp. 166–178, 2021.

[21] K. Ravikumar, K. Kiran, and V. S. Sreebalaji, "Characterization of mechanical properties of aluminium-tungsten carbide composites," *Measurement*, vol. 102, pp. 142–149, 2017.

[22] A. Mazahery and M. O. Shabani, "Microstructural and abrasive wear properties of SiC reinforced aluminum-based composite produced by compocasting," *Transactions of Nonferrous Metals Society of China*, vol. 23, no. 7, pp. 1905–1914, 2013.

[23] H. Zhou, P. Yao, T. Gong et al., "Effects of ZrO_2 crystal structure on the tribological properties of copper metal matrix composites," *Tribology International*, vol. 138, pp. 380–391, 2019.

[24] M. Narimani, B. Lotfi, and Z. Sadeghian, "Evaluation of the microstructure and wear behavior of AA6063-B_4C/TiB_2 mono and hybrid composite layers produced by friction stir processing," *Surface and Coatings Technology*, vol. 285, pp. 1–10, 2016.

[25] S. Khoshsima, S. Mertdinc, A. Motallebzadeh, Z. Altintas, D. Agaogullari, and Ö. Balcı-Çağıran, "Enhanced hardness and wear resistance of Al-based hybrid MMCs by using of composite metal boride reinforcement particles," *Materials Chemistry and Physics*, vol. 288, Article ID 126377, 2022.

[26] R. Kumar, J. Singh, S. Sharma, C. Li, G. Krolczyk, and S. Wojciechowski, "Neutrosophic entropy-based ingenious measurement for fast fourier transforms based classification of process-parameters and wear resistance of friction-stir processed hybrid AA7075- B_4C aluminium metal-matrix composites," *Journal of Materials Research and Technology*, vol. 20, pp. 720–739, 2022.

[27] G. Veeresha, B. Manjunatha, V. Bharath, M. Nagaral, and V. Auradi, "Synthesis, microstructural characterization, mechanical, fractographic and wear behavior of micro B4C particles reinforced Al2618 alloy aerospace composites," *Frattura Ed Integrità Strutturale*, vol. 16, pp. 385–407, 2022.